Journal of Catalysis **196,** 253–261 (2000)
doi:10.1006/jcat.2000.3050, available online at http://www.idealibrary.com on IDEAL®

Photocatalytic Oxidation of Toluene on Nanoscale TiO_2 Catalysts: Studies of Deactivation and Regeneration

Lixin Cao,* Zi Gao,* Steven L. Suib,*,[1] Timothy N. Obee,† Steven O. Hay,† and James D. Freihaut†

*Department of Chemistry, University of Connecticut, U-60, Storrs, Connecticut 06269-4060; and †United Technologies Research Center, 411 Silver Lane, East Hartford, Connecticut 06108

Received March 10, 2000; revised August 21, 2000; accepted August 28, 2000

Nanoscale TiO_2 catalysts prepared using a sol–gel method exhibit higher initial activity than commercially available P-25 TiO_2 for the photocatalytic oxidation of toluene. Unlike P-25 TiO_2, nonporous, nanoscale TiO_2 catalysts are composed mainly of mesopores with pore sizes in the range of 35–44 nm. Calcination at 420°C leads to agglomeration of nanoscale TiO_2 particles, formation of rutile, a decrease in pore capacity, and an enlargement of the mesopores. Catalysts treated at such a temperature display relatively low activity. Results of competitive adsorption of water and toluene on TiO_2 samples confirm that TiO_2 has a highly hydrophilic surface, which intrinsically suppresses the oxidation rate of toluene at high water content in the feed stream. Severe deactivation of TiO_2 catalysts is due to the accumulation of partially oxidized intermediates, such as benzaldehyde and benzoic acid, on active sites. Complete recovery of catalytic activity requires a regeneration temperature above 420°C. Using platinum loaded on TiO_2 results in lower oxidation rates of toluene, but facilitates the removal of poisonous intermediates from the deactivated TiO_2 surface. Kinetic studies of the deactivation process indicate that the adsorption of poisonous intermediates in the initial stage of the photocatalytic reaction is almost irreversible. The initial oxidation rates on the catalysts are proportional to their surface areas. The surface concentration of illuminated active sites on TiO_2 catalysts is estimated to be 0.85–0.96 μmol/m^2.

Key Words: **photocatalyst; nanoscale TiO_2; toluene oxidation; catalyst deactivation; catalyst regeneration.**

INTRODUCTION

Photocatalytic decomposition of air contaminants on semiconductor catalysts, such as TiO_2, is a potential technique for improving indoor air quality. Recently, a large quantity of work has been devoted to this field (1–3). Deactivation of photocatalysts has been found to be a crucial disadvantage of this technique in practice, especially for the oxidation of aromatics (4–7). The poisoning effects of partially oxidized intermediates are believed to be responsible for deactivation. In the study of photocatalytic oxidation of toluene, Ibusuki and Takeuchi (8) reported the formation of benzaldehyde in the effluent, and Luo and Ollis (5) identified benzoic acid in the extracts from deactivated catalysts with methanol. Méndez-Román and Cardona-Martínez (7) detected both benzaldehyde and benzoic acid using *in situ* FTIR. Oxygen-bearing compounds, especially benzoic acid, can cause irreversible loss in the photoactivity of TiO_2 catalysts. Another disadvantage of the use of TiO_2 catalysts is the effect of water concentration on photoactivity. Anpo *et al.* (9, 10) have claimed that the presence of water enhances the efficiency of electron–hole recombination, an unfavorable process for photocatalytic oxidation of air contaminants. Phillips and Raupp (11) have proposed that the competitive adsorption of water and organic compounds on TiO_2 surfaces may cause a loss in photoactivity at high humidity.

In the long run, commercially available P-25 TiO_2 has been found to be a practical photocatalyst for the removal of hazardous compounds from air. Recently, we reported the unique behavior of nanoscale TiO_2 catalysts with a particle size of 3–10 nm for the decomposition of 1-butene (12). The high activity of these materials results mainly from their large surface areas. In this paper, photocatalytic degradation of toluene on the nanoscale TiO_2 catalysts was studied. In particular, the deactivation process, regeneration conditions, and humidity effects on the catalysts in relation to their surface and structural properties have been investigated in detail.

EXPERIMENTAL SECTION

Catalyst Preparation

The catalysts used in this paper were obtained as follows. TiA was commercially available from Degussa P-25 TiO_2. Properties of P-25 have been characterized elsewhere (13).

TiB and TiC were prepared using a sol–gel process (12). Forty milliliters of anhydrous ethanol mixed with eight drops of concentrated hydrochloric acid (~37%) was added to dilute 8 g of $Ti[OCH(CH_3)_2]_4$. An ethanol–water

[1] To whom correspondence should be addressed. Fax: (860) 486-2981. E-mail: Suib@uconnvm.uconn.edu.

0021-9517/00 $35.00

solution (30 ml of ethanol and 30 ml of deionized distilled water) was then added dropwise and with vigorous stirring to hydrolyze the titanium isopropoxide solution. A gel was formed within a couple of minutes. Subsequently, ethanol and water were evaporated in a water bath at a temperature of 80°C. The gel was dried at 120°C in an oven overnight and became pale yellow chunks of TiO_2. Fine powders obtained by grinding TiO_2 chunks were calcined at 350°C or 420°C for 4 h to make TiB or TiC samples.

TiPt is a TiO_2 sample loaded with 0.5% Pt. The procedures for preparing TiO_2 were similar to those for TiB and TiC samples. $Pt(acac)_2$ was dissolved in an ethanol–HCl solution and deposited on TiO_2 by an incipient wetness method. This sample was finally calcined at 350°C for 4 h.

Films for activity tests were prepared by coating the above powder materials on microscope glass slides. Fifty milligrams of a sample dispersed in water was coated on each slide with an area of 13.5 cm^2 (7.5 cm × 1.8 cm). Films with such high loadings are thick enough to prevent UV light from penetrating the slides (14).

Apparatus

Oxidation rates of toluene presented in this paper were directly obtained in a glass plate photocatalytic reactor since the reactor was operated as a differential reactor under conditions of high flow rates (3.6 l/min) and low conversion of toluene (<20%). A detailed description of the reactor and its operation was presented previously (15, 16). At room temperature and approximately atmospheric pressure, the reaction rate can be expressed as

$$r_T = 0.654\chi C_{T0}/N, \quad [1]$$

where r_T in micromoles per hour per square centimeter is the oxidation rate, χ is the conversion of toluene, and C_{T0} is the inlet concentration of toluene. In this study, C_{T0} was almost always controlled at 10 ppm. N is the number of slides used for the reaction.

UV illumination was generated with a pair of black-light lamps ($\lambda > 300$ nm, 352-nm peak intensity, SpectroLine XX-15A). The UV intensity at the catalyst surface was measured with a UVA power meter (Oriel UVA Goldilux) and was 0.70 mW/cm^2. Air was passed through a water bubbler to obtain different water vapor amounts in the feed stream. The concentrations of water were measured using a humidity and temperature transmitter (Vaisala). A GC (HP-5890 II) equipped with an FID detector and an RTX-5 column (RESTEK Corp.) was used to measure the inlet and outlet concentrations of toluene.

Characterization Methods

Diffuse reflectance Fourier transform infrared (FTIR) spectroscopy experiments were performed on a Nicolet 750 spectrometer with a mercury–cadmium–telluride (MCT) detector and a KBr beam splitter. Spectra were collected with a resolution of 4 cm^{-1} using 100 scan averages.

Temperature-programmed oxidation (TPO) was used to study the carbon species on used catalysts. Fifty milligrams of sample scraped from the used TiO_2 films was loaded into a quartz reactor and purged with ultrahigh-purity helium flow. The oxidation of adsorbed carbon species was carried out using 5% oxygen in helium with a flow rate of 30 ml/min. The temperature rose linearly from 30 to 650°C. The CO_2 concentration was monitored with a mass spectrometer equipped with a quadrupole ionizing detector (MKS Instrument Inc.).

Competitive adsorption of water and toluene on the TiO_2 surface was performed in a flow-type apparatus with a fixed-bed adsorber at room temperature and atmospheric pressure. The 100-mg samples were activated at 350°C for 1 h in flowing helium. A 15 ml/min flow of helium gas was then passed through a single saturator filled with a two-phase mixture of water and toluene. The partial pressures of water and toluene were 2.31 and 2.91 kPa, respectively. A mass spectrometer was employed to monitor the concentrations of water and toluene in the stream.

Measurements of the nitrogen BET surface areas and adsorption isotherms were conducted using an ASAP 2010 instrument supplied by Micromeritics. After being degassed for 2 h at 100°C and 10 h at 300°C under vacuum, samples were cooled to ambient temperature and transferred to the adsorption port.

X-ray powder diffraction (XRD) experiments were carried out on a Scintag Model PDS 2000 diffractometer. Samples were loaded onto glass slides, and Cu $K\alpha$ radiation was used at 45 kV and 40 mA. The sample scans were collected between 5° and 80° 2θ.

RESULTS

Catalytic Activity

As we reported previously (12), nanoscale TiO_2 exhibited high reactivity in the oxidation of organic contaminants. In this study, similar catalysts were used in the degradation of toluene. The oxidation rates of toluene were based on the difference in toluene concentrations before and after UV illumination. No intermediate products, such as benzaldehyde or benzoic acid, were detected in the effluent although they were identified on the surface of used catalysts. According to Ibusuki and Takeuchi (8) and Gratson *et al.* (17), photocatalytic oxidation of aromatics primarily produced CO_2 in the effluent.

The activity of different catalysts under dry conditions is illustrated in Fig. 1. The sequence of initial oxidation rates obtained on these catalysts is TiB > TiPt > TiC > TiA. The catalyst prepared using a sol–gel method and calcined at 350°C (TiB) exhibited the highest catalytic activity

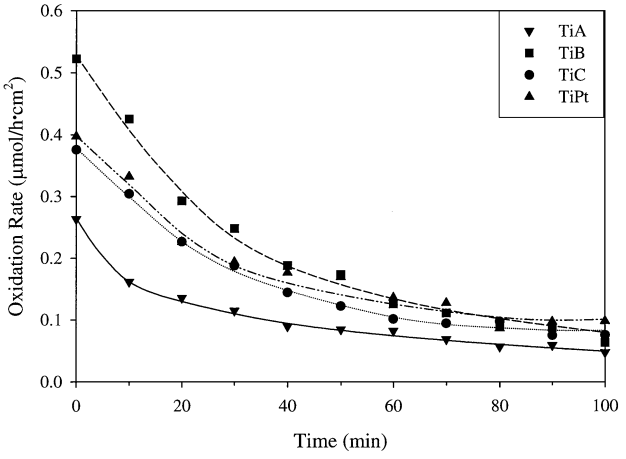

FIG. 1. Dependence of the oxidation rate of toluene versus reaction time in the absence of water vapor; $I_0 = 0.70$ mW/cm^2, flow rate = 3.6 l/min, $C_{T0} = 10$ ppm.

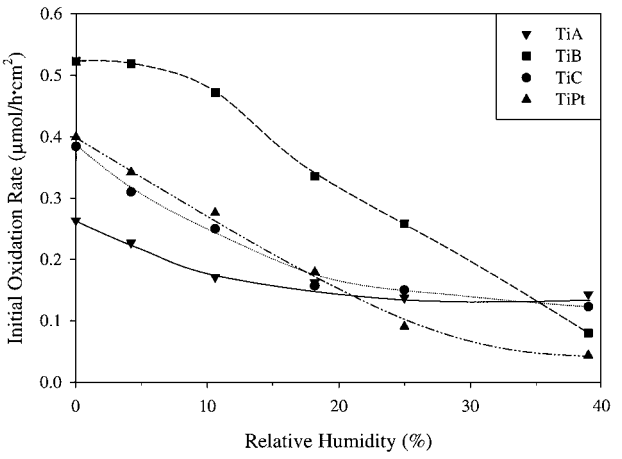

FIG. 2. Effect of water concentration on the oxidation rate of toluene; $I_0 = 0.70$ mW/cm^2, flow rate = 3.6 l/min, $C_{T0} = 10$ ppm.

(0.52 μmol/h · cm^2). XRD results shown later in this section verified that this material was a nanoscale crystal with a particle size of 7.0 nm. Loading of 0.5% Pt on this type of TiO_2 (TiPt) lowered the oxidation rate, because the presence of platinum on TiO_2 surfaces might accelerate the electron–hole recombination, an unfavorable process for photocatalysis. After being calcined at 420°C, the TiC sample exhibited an initial oxidation rate as low as 0.38 μmol/h · cm^2. Calcination of nanoscale TiO_2 at such a high temperature could cause a phase transformation (from anatase to rutile) and the agglomeration of the nanoscale particles. The commercially available P-25 TiO_2 (TiA) showed the lowest catalytic activity although it has been generally considered as a good photocatalyst and was chosen as a standard for comparison purposes in different laboratories (18). All the catalysts deactivated drastically in the initial stage and reached a relatively steady state at a fairly low oxidation rate (approximately 0.10 μmol/h · cm^2). After each test, the catalyst color changed from white to yellow, indicating that a certain amount of carbon species was deposited on the catalyst surface. These observations are consistent with what was reported in the literature (5–7).

Effect of Humidity

Many authors (9, 11, 12) have described a significant effect of humidity on the degradation rate of air contaminants. The effect of humidity on the oxidation rate of toluene is shown in Fig. 2. The initial oxidation rates decreased with an increase in water amount in the feed stream. The advantage of TiB over other catalysts in the absence of water was eliminated at high humidity (about 40%). However, the TiC sample treated at 420°C showed a stronger resistance to the negative effect of humidity. Although TiA showed low activity in the absence of water, its resistance to humidity effects is superior to that of other TiO_2 samples. In high humidity, the oxidation rates of TiC and TiA are almost identical.

The surface of TiO_2 catalysts is abundant in hydroxyl groups, which can adsorb water via hydrogen bonding or aromatics via an OH$\cdots\pi$-electron-type complex (19). The competitive adsorption of toluene and water on the catalysts was studied by measuring their hydrophobic indices (*HI*) (20, 21). *HI* is defined as the ratio of the mass of toluene to water adsorbed on the sample under competitive conditions, which is often used as a quantitative parameter for identifying the hydrophobicity or hydrophilicity of solid samples. Figure 3 shows typical breakthrough curves of toluene and water for a TiB sample. Toluene started to break through after about 6 min whereas the breakthrough time for water was as long as 22 min. The *HI* values obtained for different catalysts are listed in Table 1. Both the reaction data and competitive adsorption results indicate

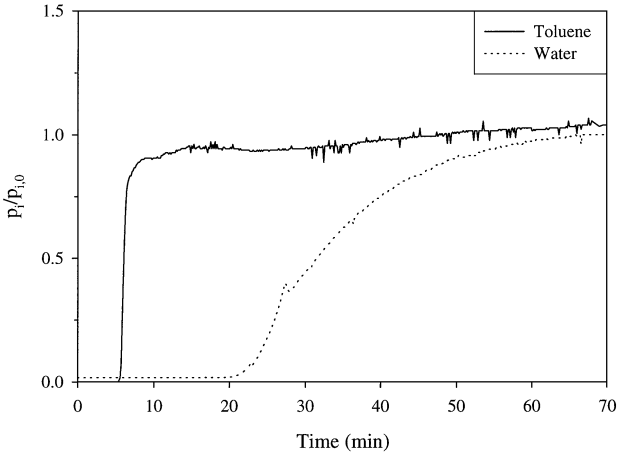

FIG. 3. Typical breakthrough curve for competitive adsorption of water and toluene on the TiB sample.

TABLE 1

Surface, Structural, and Textural Properties of TiO_2-Based Catalysts

Sample	*HI*	Surface area (m^2/g)	MPPS[a] (nm)	Average particle size (nm)	XRD results
TiA	3.2	54.6	500	28	A[b] + R[c]
TiB	2.0	105.1	36	7.0	A
TiC	2.5	77.8	44	10.1	A + R
TiPt	1.8	103.0	35	7.2	A

[a] MPPS: most possible pore size.
[b] A stands for anatase.
[c] R stands for rutile.

that catalysts with lower *HI* values seem to be more sensitive to humidity. This result confirms that the surface of the TiO_2 catalysts is strongly hydrophilic and the preferential adsorption of water on the surface is responsible for the low oxidation rate at high humidity.

Regeneration of Deactivated Catalysts

One of the disadvantages for the application of TiO_2 to photocatalytic decomposition of air contaminants is catalyst deactivation due to the strong adsorption of intermediates on active sites on the TiO_2 surface. The deactivated catalysts can be regenerated by burning out the chemisorbed carbon species in air. In this case, TiB and TiC were chosen to investigate the effect of regeneration temperature on catalytic activity. At the preparation temperatures for TiB and TiC at 350 and 420°C, respectively, both of the catalysts were regenerated in air in 2 h. The data in Figs. 4 and 5 demonstrate the effect of regeneration on the oxidation rates of TiB and TiC. The lowering of the initial

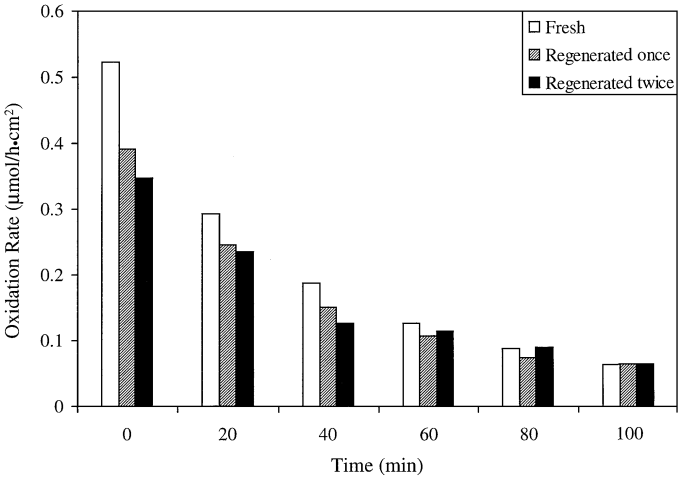

FIG. 4. Comparison of catalytic activity of the TiB sample regenerated at 350°C; $I_0 = 0.70$ mW/cm^2, flow rate = 3.6 l/min, $C_{T0} = 10$ ppm.

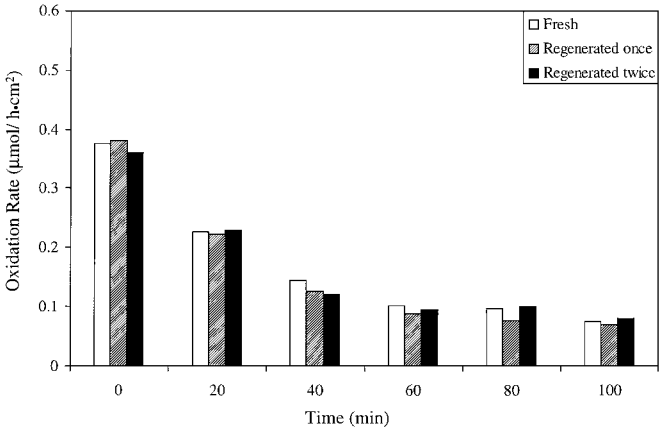

FIG. 5. Comparison of catalytic activity of the TiC sample regenerated at 420°C; $I_0 = 0.70$ mW/cm^2, flow rate = 3.6 l/min, $C_{T0} = 10$ ppm.

oxidation rate of TiB showed that the catalyst was probably partially regenerated at 350°C. In contrast, the activity of TiC was completely recovered after being regenerated at 420°C in air. As mentioned before, the catalysts turned yellow after deactivation. After being regenerated at 350°C for 2 h, the TiB sample was still light yellow. However, the TiC sample returned to its original white color after being regenerated at 420°C. Hence, 350°C is probably too low a temperature for the regeneration of these types of catalysts, and a suitable regeneration temperature is 420°C.

Temperature-Programmed Oxidation of Carbon Species

Temperature-programmed oxidation (TPO) was used to investigate the burning process of adsorbed carbon species on deactivated catalysts. Since the change in oxygen concentration was not sensitive enough to be the TPO signal in our experiments, the evolution of CO_2 from used samples was alternatively chosen to monitor the oxidation process. CO_2 evolution curves are presented in Fig. 6. Curve A indicates that the fresh TiO_2 sample prepared by a sol–gel method is free of carbon species. The curve for the TiA sample reveals three peaks at 280, 360, and 420°C, indicating that different carbon species are present on the deactivated catalyst. These carbon species are strongly adsorbed on the active sites of the TiO_2 surface, as indicated by the high burning temperatures. The curves for TiB and TiC samples exhibit highly unsymmetrical peaks at 420°C, showing that larger amounts of carbon species have been deposited on the deactivated catalysts due to their high photocatalytic activity. The curve for the TiPt sample displays a peak at 360°C and a shoulder at 280°C. The decrease of the burning temperature can be ascribed to the presence of platinum, which is known to be an excellent catalyst for complete oxidation of carbon species at low temperature. The above TPO results are consistent with those of the regeneration tests,

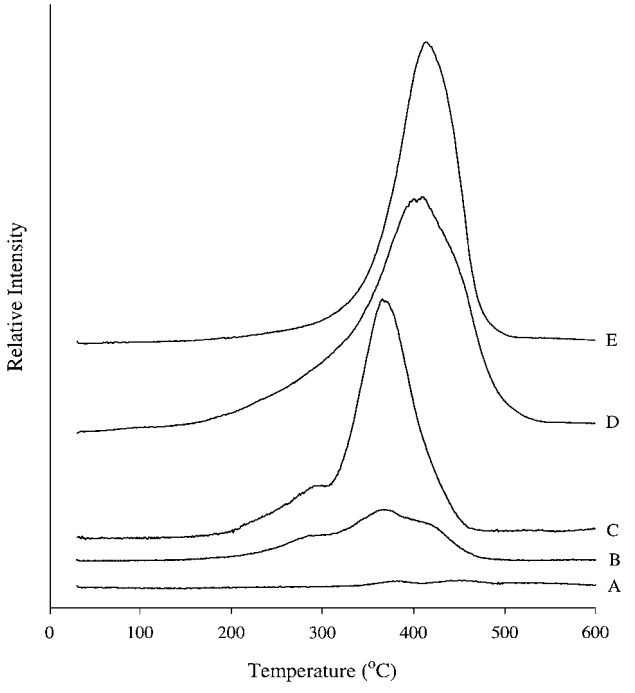

FIG. 6. Evolution of CO_2 during the temperature-programmed oxidation of carbon species on TiO_2 catalysts: (A) fresh TiB, (B) used TiA, (C) used TiPt, (D) used TiB, and (E) used TiC.

indicating that 420°C is needed to burn out all the adsorbed carbon species on the deactivated catalysts. The determination of the adsorbed species on the deactivated catalysts was carried out further by using Fourier transform infrared spectroscopy.

Fourier Transform Infrared Experiments

During the reaction, the catalysts turned from white to pale yellow gradually, and the catalyst deactivation occurred simultaneously with the color change. Méndez-Román and Cardona-Martínez (7) reported that benzaldehyde and benzoic acid were responsible for the deactivation of TiO_2-based catalysts. Ibusuki and Takeuchi (8) identified the presence of benzaldehyde in the effluent, while Luo and Ollis (5) claimed that only benzoic acid was detected in their experiments. In our study, methanol was first used to extract adsorbed oxygenates. The results of mass spectroscopic analysis indicated that the adsorbed intermediates were mainly benzaldehyde and benzoic acid, with a very small amount of benzyl alcohol. Our FTIR experiments, as shown in Fig. 7, further confirmed that irreversible adsorption of benzaldehyde and benzoic acid could occur on TiO_2 catalysts.

Spectrum A reveals that the surface of a fresh TiB catalyst is relatively clean. The band at 1623 cm^{-1} is assigned to an –OH bend corresponding to the stretch at 2500–3700 cm^{-1}. Surface changes on the fresh TiO_2 sample soaked with benzoic acid solution are indicated in spectrum F, where new bands appear at 1515, 1455, and 1417 cm^{-1}. The TiO_2 sample was further exposed to benzaldehyde for 1 h. More new bands at 1684, 1645, 1602, 1585, and 1221 cm^{-1} emerge in spectrum G. The band at 1684 cm^{-1} is assigned to a carbonyl vibration of aldehyde. The vibrations of an aromatic ring are associated with bands at 1645, 1602, and 1585 cm^{-1}. The two bands at 1520 and 1416 cm^{-1} are from the asymmetric and symmetric vibrations of the COO^- group. The detailed assignment of major IR bands is referred to in the literature (7, 22, 23). By comparing spectra B and G, it can be seen that the deactivated catalyst gives IR bands almost identical to those of the fresh TiO_2 sample treated with benzoic acid and benzaldehyde in sequence. Therefore, benzoic acid and benzaldehyde are believed to be present on deactivated catalysts. After the deactivated TiB catalyst was regenerated at 350°C for 2 h, benzoic acid remained intact on the surface as indicated by spectrum C. Spectrum E indicates that a clean surface was recovered only if the used TiO_2 catalyst was regenerated at 420°C. However, for deactivated TiPt samples the catalyst surface was free of intermediates after regeneration at 350°C as determined from spectrum D. IR results reveal that benzoic acid is more difficult to oxidize on TiO_2 surfaces than benzaldehyde. The TPO peaks at 280, 360, and 420°C of the deactivated TiO_2 catalysts can be attributed to the oxidation of adsorbed benzyl alcohol, benzaldehyde, and benzoic acid, respectively. Both the IR and TPO experiments confirm that the deactivation of this type of catalyst arises from the irreversible adsorption of reaction intermediates, such as benzaldehyde and benzoic acid. The complete removal

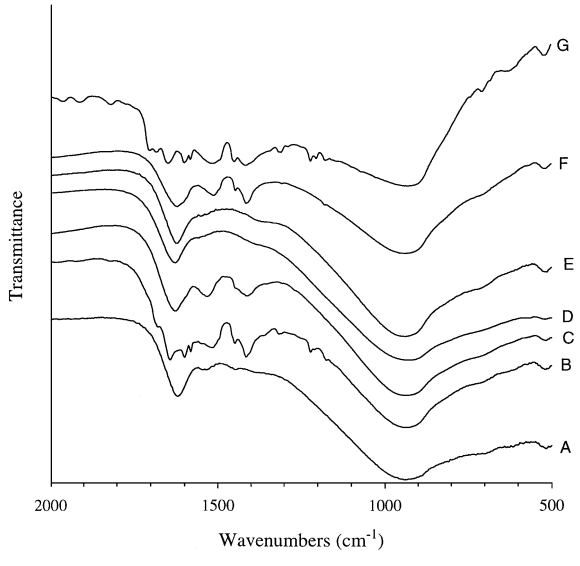

FIG. 7. Diffusion reflectance FTIR spectra: (A) fresh TiB, (B) used TiB, (C) used TiB regenerated at 350°C, (D) TiPt regenerated at 350°C, (E) TiC regenerated at 420°C, (F) TiB treated with benzoic acid, and (G) TiB treated with benzoic acid and benzaldehyde.

of these strongly adsorbed intermediates requires a burning temperature at or above 420°C.

BET, Adsorption Isotherm, and XRD Results

P-25 TiO_2 was reported to be a nonporous material with a surface area of approximately 50 m^2/g, an average particle size of 30 nm, and a mixture with anatase and rutile crystal structures (anatase : rutile ratio, 70 : 30). The unique photocatalytic activity of nanoscale TiO_2 catalysts prepared using a sol–gel method might be due to their unusual textural properties and structure. BET surface areas for those samples are listed in Table 1. The surface area of TiA (54.6 m^2/g) is close to the reported literature value, while the surface area of TiB is twice as large as that of TiA. The lower surface area of TiC is due to its higher calcination temperature (420°C), which might cause sintering, as well as collapse of the pores. The N_2 adsorption isotherms of the samples are shown in Fig. 8. The TiA curve indicates that P-25 TiO_2 is primarily composed of macropores. The maximum in pore size distribution curve of TiA is located at 500 nm. In contrast, the appearance of the hysteresis loops on the TiB and TiC curves demonstrates that these samples mainly contain mesopores with a pore size maximum of 36 and 44 nm, respectively. After being calcined at 420°C, TiC has a lower adsorption capacity, illustrated by the downward shift of the TiC curve and a larger pore size. Loading platinum did not significantly change the textural properties of TiO_2.

XRD results are listed in Table 1. The Scherrer equation (24) was used to calculate average particle sizes, more strictly, crystalline sizes. TiC has a larger particle size than TiB because of particle agglomeration caused by a higher calcination temperature. Furthermore, the appearance of rutile indicates that a phase transformation from anatase to rutile below 420°C had occurred. Rutile was claimed to be less active than anatase for the photodecomposition of hazardous compounds (25, 26). The effects of particle size on photoactivity were elucidated previously (1, 12, 16).

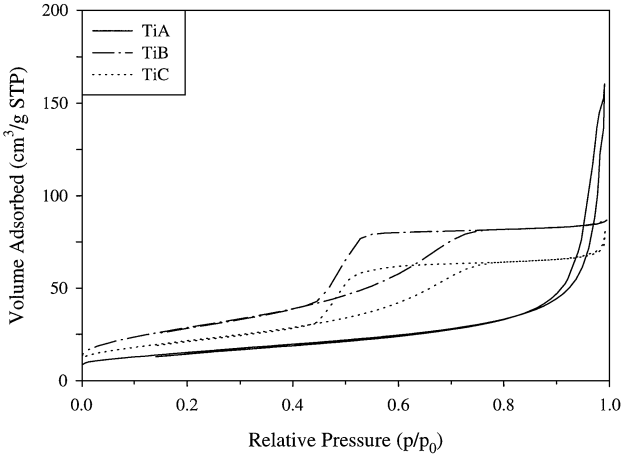

FIG. 8. N_2 adsorption isotherms of TiO_2 samples.

DISCUSSION

Catalyst deactivation during the course of photodecomposition of toluene was widely reported in the literature (4–7). The strong interaction between the active sites on the catalyst surface and the oxygen-bearing reaction intermediates leads to an abrupt decrease in the number of active sites during the course of reaction. The color change of used catalysts is directly associated with the accumulation of those intermediates on the surface. In our study, three stable reaction intermediates, benzyl alcohol, benzaldehyde, and benzoic acid, were identified on the used catalyst by extraction with methanol. IR results further confirmed the presence of benzaldehyde and benzoic acid on the catalyst surface. On the basis of the above observations, the oxidation process probably proceeded in the following sequence: toluene → benzyl alcohol → benzaldehyde → benzoic acid. The highly stable aromatic ring of toluene is intact when the active methyl group of the toluene molecule is oxidized step-by-step to benzoic acid. The formation of the carbonyl group makes the benzyl ring even more inert because the conjugation effect of the carbonyl group reduces the electron density of the benzyl ring. The complete oxidation products, such as CO_2 and water, come from any of the intermediates when the benzyl ring is broken.

Since the photocatalytic reactions are conducted at room temperature, the surface of the catalysts is gradually occupied by irreversibly chemisorbed intermediates, which retard the reaction. Regeneration of deactivated catalysts requires elevated temperatures in order to remove the intermediates from the active sites. TPO and FTIR experiments demonstrate that the burning temperatures of benzaldehyde and benzoic acid in air are 360 and 420°C, respectively. Hence, for complete recovery of deactivated catalysts, a regeneration temperature at or above 420°C is needed. However, heat treatment at 420°C may cause the phase transformation of anatase to rutile (27), and the agglomeration of the nanoscale TiO_2 particles, which are unfavorable for the photoactivity of the catalysts. Loading a small amount of platinum on TiO_2 catalysts may be a solution to this problem, because platinum is able to facilitate the combustion of the intermediates and lowers the regeneration temperature. Nevertheless, if the platinum loading of the catalyst is too high, a low regeneration temperature may be obtained at some sacrifice in the photoactivity since platinum may accelerate the recombination of electrons and holes in the photocatalytic reaction. To find an appropriate compromise between these two factors is a worthwhile project for the future.

For all the catalysts in this study, the oxidation rates decrease almost exponentially with increasing reaction time,

especially in the first hour of activity tests and under dry condition (Fig. 1). Such a common variation trend inspired us to investigate the deactivation kinetics of TiO_2 catalysts for photocatalytic oxidation of toluene. In our kinetic model, the adsorption of the poisonous intermediates, such as benzaldehyde and benzoic acid, is assumed to be irreversible. Moreover, compared to toluene adsorption, the surface reaction from adsorbed toluene to benzaldehyde or benzoic acid proceeds very fast. Thus, the conversion from gas-phase toluene molecules to intermediates can be simplified as follows:

$$T + S \xrightarrow{k_a} P \cdot S, \qquad [2]$$

where T is the gas-phase toluene, S is the active site on the catalyst surface, and $P \cdot S$ is the adsorbed poisonous intermediate. Some further definitions include

- r oxidation rate of toluene, μmol/h · g cat, which is different from r_T (μmol/h · cm^2) in Eq. [1]. $r = r_T \cdot 13.5\ cm^2/0.050$ g cat
- r_0 initial oxidation rate, μmol/h · g cat
- t reaction time, h
- k_a specific reaction rate, $(h \cdot ppm)^{-1}$
- C_S surface concentration of vacant active sites, μmol/g cat
- $C_{P \cdot S}$ surface concentration of active sites occupied by poisonous intermediates, μmol/g cat
- C_0 total surface concentration of active sites, μmol/g cat, $C_0 = C_S + C_{P \cdot S}$
- C_0' total surface concentration of active sites, μmol/m^2
- S_{BET} BET surface area, m^2/g
- P_T partial pressure of toluene in the gas phase, ppm
- a catalytic activity defined as r/r_0, time-dependent

The reaction rate (r) in our study is based on the disappearance of toluene concentration. According to Eq. [2], it can also be expressed stoichiometrically as the disappearance of vacant sites, i.e., $r = -dC_S/dt$. Equation [2] also shows that the disappearance rate of vacant sites is directly proportional to the partial pressure of toluene (P_T) and the concentration of vacant sites (C_S), i.e.,

$$-dC_S/dt = k_a P_T C_S. \qquad [3]$$

Integrating Eq. [3] with a boundary condition, $C_S = C_0$ at $t = 0$, gives us an expression for C_S:

$$C_S = C_0 \exp[-k_a P_T t]. \qquad [4]$$

Therefore, the oxidation rate can be written as

$$r = k_a P_T C_0 \exp[-k_a P_T t]. \qquad [5]$$

Plotting $\ln(r)$ against $-t$, we can obtain a straight line with an intercept of $\ln(k_a P_T C_0)$ and a slope of $k_a P_T$ for each TiO_2 catalyst (Fig. 9). The r values (μmol/h · g cat) in Fig. 9 are transferred from Fig. 1. The data points after 60 min are discarded because of deviation from linear regression. The deviation might originate from the negligence of intermediate desorption to form complete oxidation products since the desorption rate cannot be neglected in comparison with the adsorption rate in this stage. Therefore, only at the initial stage of reaction, when the adsorption of intermediates is significantly faster than their desorption, can the assumption of irreversible adsorption be correctly considered.

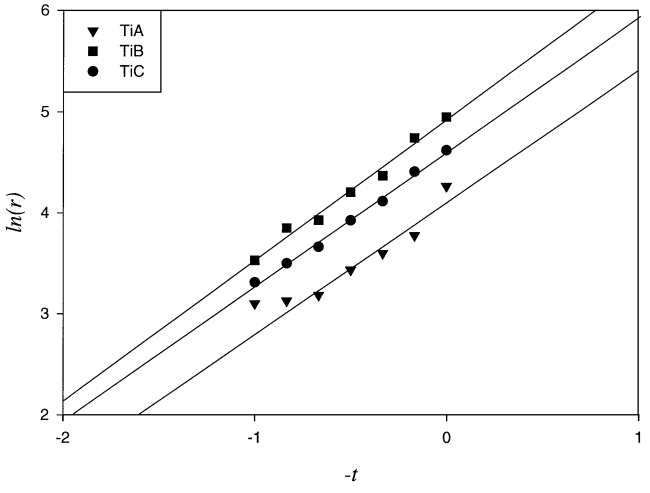

FIG. 9. Linear regression of $\ln(r)$ versus $-t$ according to Eq. [5].

From the regression results in Fig. 9, the total surface concentration of active sites C_0 can be computed via $C_0 = \exp[\text{intercept}]/\text{slope}$. C_0' expressed in micromoles per square meter is obtained from the corresponding C_0 divided by the surface area of a specific sample, i.e. $C_0' = C_0/S_{BET}$. These results are listed in Table 2. Theoretically, the C_0' values reflecting the number of active sites per area should be identical for pure TiO_2 samples with the same surface properties. The closeness of the C_0' values for different TiO_2 samples in Table 2 shows that our kinetic model for the deactivation process is creditable. Active sites mentioned here refer to illuminated active sites since the calculation of C_0 and C_0' is based on photo-oxidation rates.

The initial oxidation rate (r_0) is obtained from Eq. [5] when t is equal to zero:

$$r_0 = k_a P_T C_0 = k_a P_T C_0' S_{BET}. \qquad [6]$$

TABLE 2

Surface Concentration of Active Sites Calculated from Kinetic Model

Sample	C_0 (μmol/g)	C_0' (μmol/m^2)
TiA	46.55	0.85
TiB	98.47	0.94
TiC	74.72	0.96

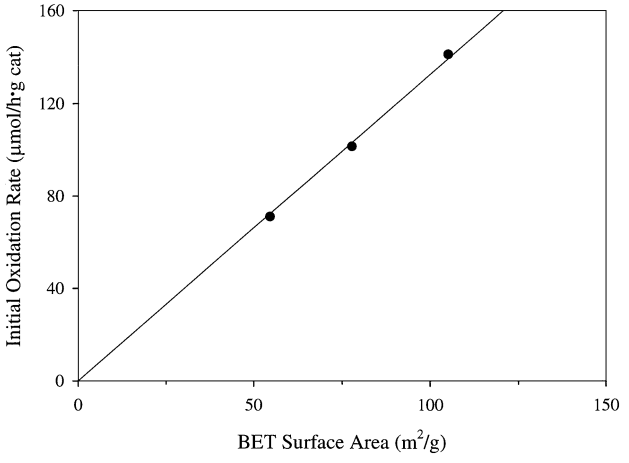

FIG. 10. Dependence of initial oxidation rates on BET surface areas according to Eq. [7].

$k_a P_T$ is a constant since the partial pressure of toluene is kept at 10 ppm, and C_0' is also a constant for pure TiO_2 samples. Thus, the initial oxidation rate can be rewritten as

$$r_0 = k' S_{BET}, \quad [7]$$

where $k' = k_a P_T C_0'$. A straight line passing through the origin should be obtained by plotting r_0 versus S_{BET}. Figure 10 verifies the reliability of this deduction. In other words, the initial oxidation rate is linearly dependent on the catalyst surface area.

Furthermore, if catalytic activity a is defined as $a = r/r_0$, the expression of a is as follows from a combination of Eqs. [5] and [6]:

$$a = \exp[-k_a P_T t]. \quad [8]$$

The rate of catalyst deactivation is defined as $r_d = -da/dt$. Thus, the expression r_d can be easily obtained by differentiating Eq. [8]:

$$r_d = -da/dt = k_a P_T a. \quad [9]$$

Obviously, in this case, the deactivation rate is first order (28).

Water concentration in the feed stream has a significant impact on the oxidation rate of toluene. Phillips and Raupp (11) suggested that water is necessary to supply hydroxyl groups depleted during the course of reaction. At high water levels, however, the competitive adsorption between water and organic contaminants on active sites gives rise to a decrease in oxidation rate. Anpo *et al.* (9, 10) have proposed that the adsorption of water on TiO_2 causes structural changes, which unfavorably enhance the recombination of photogenerated electrons and holes. Our experiments concerning the competitive adsorption of water and toluene confirm that the TiO_2 surface is highly hydrophilic because of the presence of a large amount of hydroxyl groups. Consequently, the adsorption of organic substrates on TiO_2 is inherently limited in the presence of water. To increase the hydrophobicity of the TiO_2 surface through surface modification might be a practical method for the improvement of photoactivity in the future.

CONCLUSION

The nanoscale TiB and TiC samples were found to be highly active catalysts for the photodegradation of toluene. Performing the reaction at room temperature resulted in rapid deactivation of TiO_2 catalysts due to the chemisorption of intermediates, such as benzaldehyde and benzoic acid. The color change of the catalysts from white to yellow was closely associated with the accumulation of these carbon species on the active sites. The oxidation process might follow the sequence toluene → benzyl alcohol → benzaldehyde → benzoic acid. The burning temperature of adsorbed benzoic acid on the catalyst surface was as high as 420°C. Therefore, complete recovery of catalytic activity occurred only when the regeneration temperature was at or above 420°C. Loading platinum on TiO_2 lowers the regeneration temperature considerably at the expense of some photoactivity. High humidity in the feed stream significantly inhibited the oxidation rate of toluene since water was preferentially adsorbed on the hydrophilic surface of TiO_2. Kinetic studies gave the following conclusions concerning the photocatalytic process: (a) almost irreversible adsorption of intermediates in the initial reaction stage, (b) a linear dependence of initial oxidation rates on catalyst surface areas, (c) surface concentration of illuminated active sites on TiO_2 (0.85–0.96 μmol/m^2), and (d) first-order deactivation rate. These findings may shed light on the design of new types of TiO_2 catalysts with high photoactivity.

ACKNOWLEDGMENTS

We acknowledge United Technologies Research Center for use of instrumentation. We also thank Professor Frank Galasso for helpful discussion.

REFERENCES

1. Mills, A., and Le Hunte, S., *J. Photochem. Photobiol. A: Chem.* **108**, 1–35 (1997).
2. Ollis, D. F., *in* "Photocatalytic Purification and Treatment of Water and Air" (D. F. Ollis and H. Al-Ekabi, Eds.), pp. 481–497. Elsevier, Amsterdam, 1993.
3. Hoffmann, M. R., Martin, S. T., Choi, W., and Bahnemann, D. W., *Chem. Rev.* **95**, 69–96 (1995).
4. Sauer, M. L., Hale, M. A., and Ollis, D. F., *J. Photochem. Photobiol. A: Chem.* **88**, 169–178 (1995).
5. Luo, Y., and Ollis, D. F., *J. Catal.* **163**, 1–11 (1996).
6. Larson, S. A., and Falconer, J. L., *Catal. Lett.* **44**, 57–65 (1997).
7. Méndez-Román, R., and Cardona-Martínez, N., *Catal. Today* **40**, 353–365 (1998).
8. Ibusuki, T., and Takeuchi, K., *Atmos. Environ.* **20**, 1711–1715 (1986).
9. Anpo, M., Chiba, K., Tomonari, M., Coluccia, S., Che, M., and Fox, M. A., *Bull. Chem. Soc. Jpn.* **64**, 543–551 (1991).

10. Park, D.-R., Zhang, J., Ikeue, K., Yamashita, H., and Anpo, M., *J. Catal.* **185**, 114–119 (1999).
11. Phillips, L. A., and Raupp, G. B., *J. Mol. Catal.* **77**, 297–311 (1992).
12. Cao, L., Huang, A., Spiess, F.-J., and Suib, S. L., *J. Catal.* **188**, 48–57 (1999).
13. Fox, M. A., and Dulay, M. T., *Chem. Rev.* **93**, 341–357 (1993).
14. Jacoby, W. A., Blake, D. M., Noble, R. D., and Koval, C. A., *J. Catal.* **157**, 87–96 (1995).
15. Obee, T. N., and Hay, S. O., *Environ. Sci. Technol.* **31**, 2034–2038 (1997).
16. Cao, L., Spiess, F.-J., Huang, A., Suib, S. L., Obee, T. N., Hay, S. O., and Freihaut, J. D., *J. Phys. Chem. B* **103**, 2912–2917 (1999).
17. Gratson, D. A., Nimlos, M. R., and Wolfrum, E. J., "Proc. 88th Annual Meeting of the Air and Waste Management Association," San Antonio, TX, 1995.
18. Matthews, R. W., and McEvoy, S. R., *J. Photochem. Photobiol. A: Chem.* **66**, 355–366 (1992).
19. Nagao, M., and Suda, Y., *Langmuir* **5**, 42–47 (1989).
20. Weitkamp, J., Kleinschmit, P., Kiss, A., and Berke, C. H., *in* "Proc. 9th International Zeolite Conference" (R. von Ballmmos, J. G. Higgins, and M. M. J. Treacy, Eds.), Part II, pp. 79–87. Butterworth-Heinemann, Boston, 1992.
21. Weitkamp, J., Ernst, S., Roland, E., and Thiele, G. F., *in* "Progress in Zeolite and Microporous Materials, Studies in Surface Science and Catalysis" (H. Chon, S.-K. Ihm, and Y. S. Uh, Eds.), Vol. 105, pp. 763–770. 1997.
22. Zhang, Y., Martin, A., Berndt, H., Lücke, B., and Meisel, M., *J. Mol. Catal.* **118**, 206–214 (1997).
23. Sanati, M., and Andersson, A., *J. Mol. Catal.* **81**, 51–62 (1993).
24. Azaroff, L. V., "Elements of X-Ray Crystallography," Chap. 20. McGraw-Hill, New York, 1968.
25. Mills, A., Morris, S., and Davies, R., *J. Photochem. Photobiol. A: Chem.* **70**, 183–191 (1993).
26. Martin, S. T., Morrison, C. L., and Hoffmann, M. R., *J. Phys. Chem.* **98**, 13695–13704 (1994).
27. Fu, X., Clark, L. A., Yang, Q., and Anderson, M. A., *Environ. Sci. Technol.* **30**, 647–653 (1996).
28. Fogler, H. S., "Elements of Chemical Reaction Engineering," 2nd Ed., Chap. 6, Prentice-Hall, Englewood Cliffs, NJ, 1992.